Convergence and Diversity Analysis of Indicator-based Multi-Objective Evolutionary Algorithms

Jesús Guillermo Falcón-Cardona
Computer Science Department
CINVESTAV-IPN
Mexico, Mexico City 07360
jfalcon@computacion.cs.cinvestav.mx

Carlos A. Coello Coello
Departamento de Sistemas
UAM-Azcapotzalco
Mexico, Mexico City 02200
ccoello@cs.cinvestav.mx

ABSTRACT

In recent years, quality indicators (QIs) have been employed to design selection mechanisms for multi-objective evolutionary algorithms (MOEAs). These indicator-based MOEAs (IB-MOEAs) generate Pareto front approximations that present convergence and diversity characteristics strongly related to the QI that guides the selection mechanism. However, on complex multi-objective optimization problems, the performance of IB-MOEAs is far from being completely understood. In this paper, we empirically analyze the convergence and diversity properties of five steady-state IB-MOEAs based on the hypervolume, $R2$, IGD^+, ϵ^+, and Δ_p. Regarding convergence, we analyze their speed of convergence and the final closeness to the true Pareto front. The IB-MOEAs adopted in our study were tested on problems having different Pareto front shapes, and were taken from six test suites. Our experimental results show general and particular strengths and weaknesses of the adopted IB-MOEAs. We believe that these results are the first step towards a deeper understanding of the behavior of IB-MOEAs.

CCS CONCEPTS

• **Theory of computation → Bio-inspired optimization**; • **Computing methodologies → Continuous space search**;

KEYWORDS

Multi-objective Optimization, Quality Indicators, Selection Mechanisms

ACM Reference Format:
Jesús Guillermo Falcón-Cardona and Carlos A. Coello Coello. 2019. Convergence and Diversity Analysis of Indicator-based Multi-Objective Evolutionary Algorithms. In *GECCO '19: Genetic and Evolutionary Computation Conference, July 13–17, 2018, Prague, Czech Republic.* ACM, New York, NY, USA, 8 pages. https://doi.org/10.1145/3205455.3205463

1 INTRODUCTION

Many scientific and engineering problems can be formulated in terms of the simulatenous optimization of several, often conflicting, objective functions. These are the so-called multi-objective optimization problems (MOPs), which are formally defined as follows:

$$\min_{\vec{x}\in\Omega} \left\{\vec{F}(\vec{x}) = (f_1(\vec{x}), f_2(\vec{x}), \ldots, f_m(\vec{x}))\right\} \tag{1}$$

where $\vec{x}$ is the vector of decision variables, $\Omega \subseteq \mathbb{R}^n$ is the feasible region set and $\vec{F}(\vec{x})$ is the vector of $m \geq 2$ objective functions where $f_i : \mathbb{R}^n \to \mathbb{R}$ for $i = 1, \ldots, m$. Due to the conflict among the objective functions, solving an MOP involves finding the best possible trade-offs among them. The particular set that yields the optimum values, according to the Pareto dominance relation[1], for all the objective functions is known as the Pareto optimal set and its image is known as the Pareto optimal front ($\mathcal{PF}^*$).

Multi-objective evolutionary algorithms (MOEAs) have become an increasingly popular choice to tackle complex MOPs [5]. Due to the wide variety of currently proposed MOEAs, an important issue is how to assess their performance. In the early years of MOEAs, researchers only performed qualitative comparisons of convergence and diversity (distribution and spread) of the Pareto front approximations produced by an MOEA. However, in the late 1990s, quality indicators (QIs) were proposed to compare the performance of MOEAs in a quantitative way [20]. QIs are functions that assign a real value to one or more approximated Pareto fronts, depending on their specific preferences. In consequence, they impose a total order between approximation sets [24]. Due to this order property, QIs are especially noteworthy when the Pareto dominance relation, which is the more general assumption of quality, is not enough to discriminate approximation sets.

Throughout the years, some studies on QIs have been proposed. Zitzler *et al.* [24] provided the first theoretical analysis of QIs, using a mathematical framework to understand how QIs are related to a set of outperformance relations and what type of conclusions can be drawn from them. The authors emphasized that the choice of QIs to compare MOEAs depends strongly on the type of statements that one would like to make, attending the decision maker's preferences. Jiang *et al.* [15] empirically analyzed the preferences of a set of QIs when assessing convex and concave Pareto fronts with different distributions. The authors showed the consistencies and contradictions between QIs, which was the first step to understand their relationship. In order to get a more in-depth understanding of the relationship between QIs, Liefooghe and Derbel [17] performed a correlation analysis of the way in which QIs rank approximation sets with different geometries. Due to the specific preferences of

GECCO '19, July 13–17, 2018, Prague, Czech Republic

ACM ISBN 978-1-4503-5618-3/18/07…$15.00
https://doi.org/10.1145/3205455.3205463

[1] Given $\vec{x}, \vec{y} \in \mathbb{R}^n$ and $\vec{F} : \mathbb{R}^n \to \mathbb{R}^m$, we say that $\vec{x}$ Pareto dominates $\vec{y}$ (denoted as $\vec{F}(\vec{x}) \prec \vec{F}(\vec{y})$) if and only if $\forall i = 1, \ldots, m, f_i(\vec{x}) \leq f_i(\vec{y})$ and there exists at least an index $j \in \{1, \ldots, m\}$ such that $f_j(\vec{x}) < f_j(\vec{y})$.

each QI, no pair obtains the same ranking of Pareto front approximations. Hence, their main result was to establish the degree of compliance between the adopted QIs.

Recently, QIs have motivated the design of selection mechanisms of MOEAs, giving rise to the so-called indicator-based MOEAs (IB-MOEAs). From the plethora of QIs currently available (see [16, 18]), those focused on assessing convergence have attracted particular interest since finding a set of solutions that optimize their value will produce an approximation set closer to $\mathcal{PF}^*$. The hypervolume indicator (HV) [23] has been extensively used in IB-MOEAs due to its nice mathematical properties. HV measures the volume dominated by an approximation set, being the most remarkable convergence QI because, from all the classical indicators, it is the only one that is Pareto-compliant[2]. However, its computational cost increases super-polynomially with the number of objectives. In consequence, other less expensive convergence QIs such as R2 [2], Inverted Generational Distance plus (IGD^+) [13], the additive ϵ indicator (ϵ^+) [24], and the averaged Hausdorff distance (Δ_p) [19], have been employed to guide the selection mechanisms of IB-MOEAs. Despite the wide variety of IB-MOEAs in the specialized literature, there is no clear understanding of their convergence and diversity properties when tackling MOPs with distinct Pareto front geometries and difficulties. In this paper, we perform a comprehensive empirical study of the convergence and diversity properties of five steady-state IB-MOEAs based on HV, R2, IGD^+, ϵ^+, and Δ_p. We aim to provide a first insight into the strengths and weaknesses of IB-MOEAs when tackling a wide variety of MOPs from the test suites Deb-Thiele-Laumanns-Zitzler (DTLZ) [7], Walking-Fish-Group (WFG) [12], Lamé Superspheres [8], Viennet problems (VIE) [21], and the recently proposed $DTLZ^{-1}$ and WFG^{-1} [14].

The remainder of this paper is organized as follows. Section 2 briefly introduces the selected QIs and the generic steady-state IB-MOEA employed in our study. The convergence and diversity analysis are described in Section 3. Finally, Section 4 presents the conclusions of the paper and some possible future research paths.

2 BACKGROUND

In this section, we formally define the HV, R2, IGD^+, ϵ^+, and Δ_p indicators. In all cases, let $\mathcal{A}$ be an approximation set and $\mathcal{Z}$ be a reference set. m is the dimension of the objective space. Additionally, we introduce the generic steady-state IB-MOEA, based on the framework of the S-Metric Selection Evolutionary Multi-Objective Algorithm (SMS-EMOA) [1].

2.1 Quality indicators

Definition 1 (Hypervolume indicator). *Given an anti-optimal reference point $\vec{r} \in \mathbb{R}^m$, the hypervolume is defined as follows:*

$$HV(\mathcal{A}, \vec{r}) = \mathcal{L}\left(\bigcup_{\vec{a}\in\mathcal{A}} \left\{\vec{b} \mid \vec{a} \prec \vec{b} \prec \vec{r}\right\}\right), \tag{2}$$

where $\mathcal{L}(\cdot)$ denotes the Lebesgue measure in $\mathbb{R}^m$.

[2]Let $\mathcal{A}, \mathcal{B} \subset \mathbb{R}^k$, $|\mathcal{A}| = |\mathcal{B}| = \mu$ be two approximation sets and $I : \mathbb{R}^k \to \mathbb{R}$ be a unary QI. Then, I is Pareto-compliant if $\mathcal{A} \prec \mathcal{B} \Rightarrow I(\mathcal{A}) > I(\mathcal{B})$, supposing a greater indicator value is better.

Definition 2 (Unary R2 indicator). *The unary R2 indicator is defined as follows:*

$$R2(\mathcal{A}, W) = -\frac{1}{|W|} \sum_{\vec{w}\in W} \max_{\vec{a}\in\mathcal{A}} \{u_{\vec{w}}(\vec{a})\}, \tag{3}$$

where W is a set of weight vectors and $u_{\vec{w}} : \mathbb{R}^m \to \mathbb{R}$ is a scalarizing function defined by $\vec{w} \in W$ that assigns a real value to each m-dimensional vector.

Definition 3 (IGD^+ indicator). *The IGD^+, for minimization, is defined as follows:*

$$IGD^+(\mathcal{A}, Z) = \frac{1}{|Z|} \sum_{\vec{z}\in Z} \min_{\vec{a}\in\mathcal{A}} d^+(\vec{a}, \vec{z}), \tag{4}$$

where $d^+(\vec{a}, \vec{z}) = \sqrt{\sum_{k=1}^{m} (\max\{a_k - z_k, 0\})^2}$.

Definition 4 (Unary ϵ^+ indicator).

$$\epsilon^+(\mathcal{A}, \mathcal{Z}) = \max_{\vec{z}\in\mathcal{Z}} \min_{\vec{a}\in\mathcal{A}} \max_{1\le i\le m} \{z_i - a_i\}. \tag{5}$$

The unary ϵ^+-indicator gives the minimum distance by which a Pareto front approximation needs to or can be translated in each dimension in objective space such that a reference set is weakly dominated.

Definition 5 (Averaged Hausdorff Distance (Δ_p)). *For a given $p > 0$, the Δ_p is defined as follows:*

$$\Delta_p(\mathcal{A}, Z) = \max\left\{GD_p(\mathcal{A}, Z), IGD_p(\mathcal{A}, Z)\right\}. \tag{6}$$

Δ_p is defined on the basis of two indicators: GD_p and IGD_p which are slight modifications of the indicators Generational Distance (GD) [20] and Inverted Generational Distance (IGD) [4], respectively. These are defined in the following:

Definition 6 (GD_p indicator).

$$GD_p(\mathcal{A}, \mathcal{Z}) = \left(\frac{1}{|\mathcal{A}|} \sum_{\vec{a}\in\mathcal{A}} d(\vec{a}, \mathcal{Z})^p\right)^{1/p}, \tag{7}$$

where $d(\vec{a}, \mathcal{Z}) = \min_{\vec{z}\in\mathcal{Z}} \sqrt{\sum_{i=1}^{m} (a_i - z_i)^2}$.

Definition 7 (IGD_p indicator).

$$IGD_p(\mathcal{A}, \mathcal{Z}) = GD_p(\mathcal{Z}, \mathcal{A}) = \left(\frac{1}{|\mathcal{Z}|} \sum_{\vec{z}\in\mathcal{Z}} d(\vec{z}.\mathcal{A})^p\right)^{1/p}, \tag{8}$$

Definition 8 (Indicator contribution). *Let $\mathcal{I}$ be any indicator in the set $\{HV, R2, IGD^+, \epsilon^+, \Delta_p\}$. The individual contribution C of a solution $\vec{a} \in \mathcal{A}$ to the indicator value is given as follows:*

$$C_{\mathcal{I}}(\vec{a}, \mathcal{A}) = |\mathcal{I}(\mathcal{A}) - \mathcal{I}(\mathcal{A} \setminus \{\vec{a}\})|. \tag{9}$$

2.2 Steady-state IB-MOEAs

From the large spectrum of IB-MOEAs, the one that has received particular attention is SMS-EMOA [1]. This is a steady-state MOEA that employs Pareto dominance as its main selection criterion, and it adopts a density estimator based on HV. Algorithm 1 shows the general framework of SMS-EMOA that can be adapted to any of the QIs defined in the previous section. The main loop of the generic steady-state IB-MOEA is in lines 2 to 11. At each iteration, a single

solution is created from the population P using genetic operators. This solution is then temporarily added to P to form the population Q in line 4, Then, Q is divided into a set of layers $R_1, \ldots, R_t$, using the nondominated sorting algorithm [6], where R_t contains the worst solutions according to the Pareto dominance relation. If R_t has more than one solution, an indicator-based density estimator (IB-DE) is executed. First, an IB-DE calculates the individual indicator contributions of all solutions in a given set using Eq. (9), and, finally, it deletes the solution having the minimum contribution. Regarding SMS-EMOA, its IB-DE calculates the individual contributions to HV. Finally, the IB-MOEA returns the population P as the approximation to the Pareto front. Based on the SMS-EMOA framework, other IB-MOEAs using the indicators R2 and IGD^+ have been proposed, i.e., the R2-EMOA [3] and the IGD^+-based Many-Objective Evolutionary Optimizer (IGD^+-MaOEA) [10], respectively.

Algorithm 1 Generic steady-state IB-MOEA

Require: Indicator I
Ensure: Pareto front approximation
1: Randomly initialize population P
2: **while** stopping criterion is not fulfilled **do**
3: Generate offspring $\vec{q}$ from population P
4: $Q \leftarrow P \cup \{\vec{q}\}$
5: Obtain $\vec{z}^*$ and $\vec{z}^{\text{nad}}$ from Q and normalize it
6: $\{R_1, \ldots, R_t\} \leftarrow NDsorting(Q)$
7: **if** $|R_t| > 1$ **then**
8: $\vec{r}_{\text{worst}} \leftarrow \arg\min_{\vec{r} \in R_t} C_I(\vec{r}, R_t)$
9: **else**
10: $\vec{r}_{\text{worst}}$ is the single solution in R_t
11: $P \leftarrow Q \setminus \{\vec{r}_{\text{worst}}\}$
12: **return** P

Table 1: MOPs adopted in our study. For each case, the Pareto front geometry is described, indicating whether it is correlated or not with the shape of a simplex.

MOP	Pareto front shape	Simplex-like
DTLZ5	Degenerate	✗
$DTLZ5^{-1}$	Convex	✗
DTLZ7	Disconnected	✗
$DTLZ7^{-1}$	Disconnected	✗
WFG1	Mixed	✓
$WFG1^{-1}$	Mixed	✗
WFG2	Disconnected	✓
$WFG2^{-1}$	Slightly concave	✗
WFG3	Degenerate	✗
$WFG3^{-1}$	Linear	✗
Lamé $\gamma = 0.25$	Highly convex	✗
Lamé $\gamma = 0.50$	Convex	✓
Lamé $\gamma = 1.00$	Linear	✓
Lamé $\gamma = 2.00$	Concave	✓
Lamé $\gamma = 5.00$	Highly concave	✓
Mirror $\gamma = 0.25$	Highly concave	✗
Mirror $\gamma = 0.50$	Concave	✗
Mirror $\gamma = 1.00$	Linear	✗
Mirror $\gamma = 2.00$	Convex	✗
Mirror $\gamma = 5.00$	Highly convex	✗
VIE1	Convex	✗
VIE2	Mixed (convex and degenerate)	✗
VIE3	Degenerate	✗

3 EXPERIMENTAL RESULTS

In this section, we empirically analyze the convergence and diversity properties of five steady-state IB-MOEAs, following the framework of Algorithm 1, based on the indicators HV, R2, IGD^+, ϵ^+, and Δ_p. In other words, we compare SMS-EMOA [1], R2-EMOA [3], IGD^+-MaOEA [10], and we propose ϵ^+-MaOEA and Δ_p-MaOEA. We adopted the DTLZ, WFG, VIE, Lamé superspheres, $DTLZ^{-1}$, and WFG^{-1} test suites with two and three objective functions. Table 1 describes the MOPs employed in the study, emphasizing their Pareto front geometry and whether $\mathcal{PF}^*$ is correlated with the shape of a simplex formed by a set of convex weight vectors[3]. In all cases, we performed 30 independent executions of each algorithm with each test instance.

3.1 Parameters settings

For a fair comparison, in all the experiments, the IB-MOEAs used the same population size $\mu = C_{m-1}^{H+m-1}$ which is equal to the number of convex weight vectors employed by R2-EMOA. H is a parameter that controls the number of convex weight vectors [22]. Hence, μ is equal to 100 and 105 for two and three objectives, respectively. We adopted a maximum number of function evaluations as the stopping criterion which was set to 50,000 and 60,000 for two and three objectives, respectively. All the IB-MOEAs employed simulated binary crossover and polynomial-based mutation as their genetic operators [6]. For all the objectives, the crossover and mutation probabilities were set to 0.9 and $1/n$, respectively, where n is the number of decision variables. Both the crossover and the mutation distribution indexes were set equal to 20. At each iteration, SMS-EMOA employs the vector of worst objective values of the population as the reference point of HV and the layer R_1 as the reference set in $\{IGD^+, \epsilon^+, \Delta_p\}$-MaOEA. Regarding the MOPs, the number of decision variables of problems DTLZ, $DTLZ^{-1}$, and Lamé superspheres is $n = m + K - 1$, where $K = 10$ for DTLZ5 and $DTLZ5^{-1}$; $K = 20$ for DTLZ7 and its minus version; and, $K = 5$ for the Lamé and Mirror problems that are determined by a different γ value in Table 1. Considering the WFG and WFG^{-1} test instances, n was set to 24 and 26 for two and three objective functions, respectively. In both cases, the number of position-related parameters is two. The decision space of the three VIE problems is of dimension two.

3.2 Convergence analysis

The goals of our convergence analysis are twofold. First, investigate the percentage of successful executions (denoted as "hit rate") on

[3] A vector $\vec{w} \in \mathbb{R}^m$ is a convex weight vector if and only if $\sum_{i=1}^{m} w_i = 1$ and $w_i \geq 0$, $\forall i = 1, \ldots, m$

which an IB-MOEA is sufficiently close (attending a specific criterion) to $\mathcal{PF}^*$, and, on average, how many function evaluations are required to fulfill this condition (convergence speed). Secondly, evaluate the final Pareto front approximations generated by the adopted IB-MOEAs, using multiple convergence QIs.

Regarding the former goal, we claim that an IB-MOEA is close enough to a reference set[4] $\mathcal{Z} \subset \mathcal{PF}^*$ if its population at some iteration t meets the following criterion (called ϵ^+-convergence): $\epsilon^+(P_t, \mathcal{Z}) \leq \bar{\epsilon}$, where $\bar{\epsilon}$ is a parameter set to 0.05 and 0.1 for two and three objectives, respectively. If the IB-MOEA has ϵ^+-convergence, that execution is marked as successful; otherwise, the execution is marked as failed. The hit rate (h_r) is the number of successful cases divided by the total number of executions (30 in our experiments). We take the speed of convergence as the mean value at which an IB-MOEA reaches ϵ^+-convergence. Table 2 shows the hit rate and speed of convergence for each MOP of all IB-MOEAs. The fastest IB-MOEA is shown in grayscale, and the symbol # is placed when its speed of convergence is significantly better than the other IB-MOEAs based on a one-tailed Wilcoxon test, using a significance level of $\alpha = 0.05$. From the table, it is possible to establish the strengths and weaknesses of the IB-MOEAs. We express as a general strength those test instances where all the IB-MOEAs have $h_r = 1.0$ (denoted by the symbol ✓), and a general weakness is where all the IB-MOEAs have the symbol ✗related to $h_r = 0.0$.

On the one hand, Lamé and Mirror problems, DTLZ5 in both objective dimensions, DTLZ7^{-1} 2D, WFG2^{-1} 2D, VIE2 and VIE3 are the general strengths of the adopted IB-MOEAs. On the other hand, DTLZ5^{-1} 3D, DTLZ7 3D, all WFG1 and WFG1^{-1} test instances, WFG2 2D and WFG3^{-1} 3D are considered as the general weaknesses. Figure 1 supports our claim of general weaknesses since it shows the IB-MOEAs' median ϵ^+ convergence graphs for all the above-mentioned problems. From this figure, we can see that no IB-MOEA reaches the ϵ^+-convergence condition because in some cases (DTLZ5^{-1} 3D and DTLZ7 3D) the IB-MOEAs get stuck in a higher ϵ^+ value, or the algorithms' behavior is particularly chaotic (WFG1^{-1} 2D, WFG1^{-1} 3D and WFG^{-1} 3D). Considering the 23 MOPs belonging to the DTLZ, DTLZ^{-1}, WFG, WFG^{-1} and VIE test suites (which are more difficult problems than the Lamé superspheres where all the IB-MOEAs achieved ϵ^+-convergence), IGD$^+$-MaOEA ϵ^+-converged in the largest number of MOPs (i.e., 14 problems) although SMS-EMOA and ϵ^+-MaOEA also showed outstanding results since they ϵ^+-converged in 12 and 13 test instances, respectively. Taking into account the total number of MOPs having $h_r = 0.0$ and $h_r \in (0, 1)$, Δ_p-MaOEA and R2-EMOA are the worst IB-MOEAs, having a total of 13 and 15 MOPs under these conditions, respectively. In general, SMS-EMOA presents the best results regarding the speed of convergence because, considering all the MOPs, it was the fastest in 20 out of 43 problems. Additionally, SMS-EMOA and IGD$^+$-MaOEA ϵ^+-converged in a similar number of cases. Consequently, the latter IB-MOEA can be considered to obtain ϵ^+-convergence at a lower computational cost and obtaining similar results to SMS-EMOA. In terms of ϵ^+-convergence, R2-EMOA is the worst IB-MOEA when tackling MOPs having non-simplex-like Pareto fronts. Although in Mirror problems it always presents ϵ^+-convergence, the diversity of solutions is not good, since there is a strong bias to the boundaries of the Pareto fronts. This bad performance is explained by the use of convex weight vectors. Recently, Ishibuchi *et al.* [14] empirically showed that MOEAs using convex weight vectors do not perform very well when tackling MOPs whose Pareto front shapes are not correlated to the geometry of a simplex. In our experiments, most of the problems are not correlated with the simplex shape.

To analyze the final convergence quality of the IB-MOEAs, we decided to employ the Hausdorff distance (HD) which is a well-known metric as well as the QIs: HV, R2, IGD$^+$, ϵ^+, and Δ_p. The reason to use HD is due to its neutrality when assessing the IB-MOEAs, i.e., none of them employ HD in their selection mechanism. Considering the QIs, we opted for a neutral comparison. If we compare a set of IB-MOEAs, using an indicator $\mathcal{I}$, where one of the algorithms uses $\mathcal{I}$ in its selection mechanism, the comparison will be biased to this particular IB-MOEA. Hence, we leave aside that algorithm when comparing with $\mathcal{I}$. For example, if we compare the IB-MOEAs using HV, SMS-EMOA does not take part in the comparison. Due to space limitations[5], we only present the numerical results for HD in Table 3. However, we summarize in Fig. 2 the counting of the first and second places obtained by the IB-MOEAs on the QIs. Based on HD, Δ_p-MaOEA and SMS-EMOA are the best IB-MOEAs because they obtained very similar results: the former is the best in 16 MOPs while the latter gets the first place in 15 test instances. ϵ^+-MaOEA is ranked as the worst algorithm since it only obtained the first place in one MOP, namely WFG3 3D. It is worth noting that although the behavior of Δ_p-MaOEA was not very good with regard to the hit rate and speed of convergence (as it is the case of ϵ^+-MaOEA), it obtains good results on the basis of HD. Based on this and the complete analysis of final convergence, it is possible to see that not always the fastest algorithm obtains the best final convergence performance. Hence, we believe that the hit rate and convergence speed can provide valuable insights about the exploration ability of the corresponding IB-DEs, while the final convergence results help us to determine what is the exploitation (or refinement of the approximated Pareto fronts) ability associated with the IB-DEs. To support this fact, from Figure 2, we observe that SMS-EMOA is the best algorithm for IGD$^+$, ϵ^+, and Δ_p; while Δ_p-MaOEA is the best for HV and R2. Considering the second places on each QI, we have IGD$^+$-MaOEa for HV, SMS-EMOA for R2, ϵ^+-MaOEA regarding IGD$^+$, IGD$^+$-MaOEA for ϵ^+, and, finally, R2-EMOA for Δ_p. Due to the high correlation between HV and ϵ^+ [17], and HV with IGD$^+$ [10], it is clear why SMS-EMOA significantly outperforms the other IB-MOEAs on these QIs. Additionally, the first place of SMS-EMOA in Δ_p is due to its good distribution of solutions (which is discussed in the next section) in comparison to the uniformity of solutions produced by R2-EMOA, IGD$^+$-MaOEA, and ϵ^+-MaOEA. On the other hand, Δ_p-MaOEA obtains the first place in HV because its spread and uniformity of solutions are better than that of the other IB-MOEAs, which is something rewarded by HV. The same arguments hold for the case of R2, which is also highly correlated with

[4]For each MOP, we uniformly sampled its $\mathcal{PF}^*$ to generate the reference set. The cardinality of the reference sets was set to 200 and 300 for two- and three-dimensional MOPs.

[5]The complete study can be found in http://computacion.cs.cinvestav.mx:/~jfalcon/IB-MOEAs/Study.html.

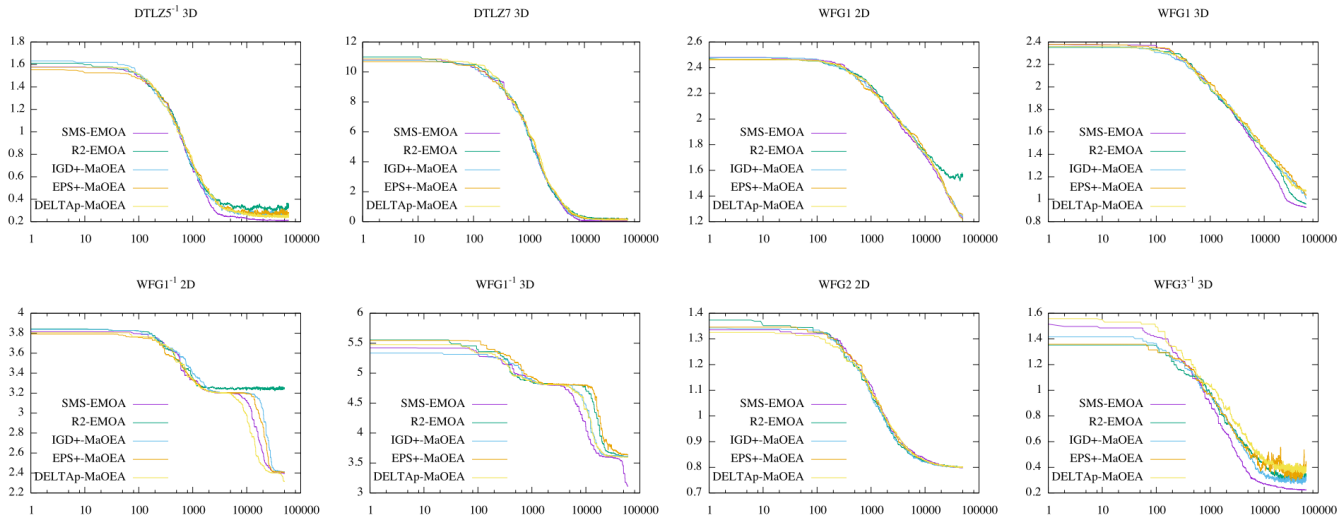

Figure 1: Convergence graphs for MOPs which represent general weaknesses for all the adopted IB-MOEAs. The x-axis is related to the number of iterations and the y-axis is the ϵ^+ value.

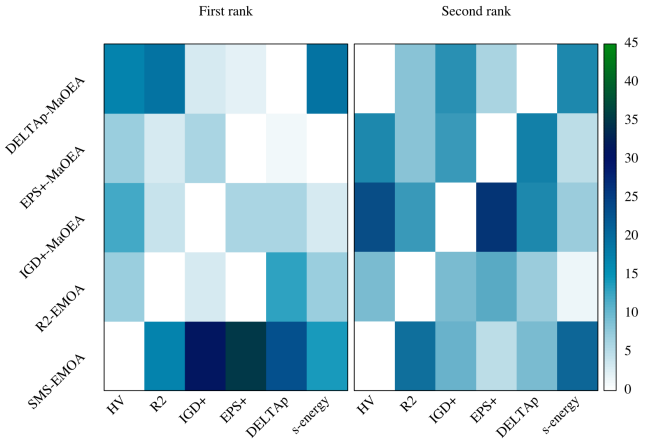

Figure 2: Heat map that shows the number of times an IB-MOEA was ranked first or second, according to the indicators HV, R2, IGD$^+$, ϵ^+, Δ_p, and s-energy.

HV although it prefers uniformly distributed solutions on linear and concave Pareto fronts.

Based on the experimental results of both experiments, the following conclusions are drawn. The IGD$^+$-based or the ϵ^+-based density estimators (DEs) can be plugged onto MOEAs to provide a higher probability to obtain ϵ^+-convergence although at a slower rate. The HV-DE is better if we are interested in a faster convergence. However, we have to consider that the cost of repeatedly computing HV contributions is time-consuming since the cost of HV increases super-polynomially with the number of objective functions. In order to refine the Pareto fronts produced by the recommended IB-DEs, we can choose Δ_p-DE since it provided excellent final convergence results regarding HD, HV, and R2. On the other hand, due to the use of convex weight vectors, R2-EMOA arises as the worst option when the Pareto front of the MOP is not correlated with the shape of a simplex. This result is supported in [14]. The rest of IB-MOEAs are not strongly sensitive to the Pareto front geometry.

3.3 Diversity analysis

To assess the diversity of solutions in the outcomes of IB-MOEAs, we decided to employ two QIs: the Solow-Polasky Diversity indicator (SPD) [9] and the Riesz s-energy indicator (E_s) [11]. Due to space limitations, we only show the numerical results of SPD in Table 4 and, in Fig. 2, we summarize the E_s results. Both SPD and E_s values show evidence that Δ_p-MaOEA produces Pareto front approximations with high diversity. In the second place, we have SMS-EMOA for both QIs as well. ϵ^+-MaOEA has the worst diversity results since it does not produce the best value in any of the test cases adopted. The results of ϵ^+-MaOEA can be explained by the fact that ϵ^+ exclusively assesses convergence while the other indicators adopted in our study simultaneously assess convergence and diversity. Hence, the ϵ^+-based DE only promotes convergence. On the other hand, from Table 4, it is easy to see that in most cases where Δ_p-MaOEA obtains the best value, such results are related to MOPs with Pareto fronts not correlated with the form of a simplex, such as DTLZ5 3D, DTLZ7 3D, WFG2^{-1} 3D and all the VIE problems. Regarding the Lamé problems, SMS-EMOA has the best results on the convex and linear instances, while R2-EMOA performs better in concave Pareto fronts. This behavior holds on the Mirror problems. In Figure 3, we show some Pareto fronts produced by the IB-MOEAs to support our claims. For instance, no IB-MOEA was able to generate the complete front of WFG1 2D (that is why this problem was highlighted as a general weakness in the previous section). Also, in the Lamé $\gamma = 2.0$ with three objectives, R2-EMOA produces evenly distributed solutions while for its mirror version, it fails to cover the entire Pareto front. For this latter problem, we

Table 2: Hit rate and, in paretheses, the mean value at which IB-MOEAs achieved ϵ^+-convergence (NA means no convergence). The symbols ✓and ✗denote hit rate values of 1.0 and 0.0, respectively.

MOP	Dim.	SMS-EMOA	R2-EMOA	IGD$^+$-MaOEA	ϵ^+-MaOEA	Δ_p-MaOEA
DTLZ5	2	✓ (1.7953e+03)	✓ (1.7531e+03)	✓ (1.7720e+03)	✓ (1.7342e+03)	✓ (1.9022e+03)#
	3	✓ (1.2437e+03)#	✓ (1.1537e+03)	✓ (1.1612e+03)	✓ (1.2500e+03)	✓ (1.2542e+03)
DTLZ5^{-1}	2	✓ (4.6186e+03)	0.03 (2.2050e+02)	✓ (4.7308e+03)	✓ (4.6646e+03)	✓ (4.8778e+03)
	3	✗ (NA)	✗ (NA)	✗ (NA)	✗ (NA)	✗ (NA)
DTLZ7	2	✓ (6.9824e+03)	✓ (7.0057e+03)	✓ (7.1448e+03)	0.97 (6.7282e+03)	✓ (7.3211e+03)#
	3	0.93 (7.8334e+03)	0.90 (1.1067e+04)	0.87 (1.3126e+04)	0.87 (1.5227e+04)	0.93 (1.6307e+04)
DTLZ7^{-1}	2	✓ (7.1510e+03)	✓ (7.4723e+03)	✓ (7.1924e+03)	✓ (7.2936e+03)	✓ (7.1836e+03)
	3	0.93 (8.9018e+03)	✓ (1.2634e+04)	0.97 (1.1393e+04)	0.93 (1.2545e+04)	0.93 (1.3663e+04)
WFG1	2	✗ (NA)	✗ (NA)	✗ (NA)	✗ (NA)	✗ (NA)
	3	✗ (NA)	✗ (NA)	✗ (NA)	✗ (NA)	✗ (NA)
WFG1^{-1}	2	✗ (NA)	✗ (NA)	✗ (NA)	✗ (NA)	✗ (NA)
	3	✗ (NA)	✗ (NA)	✗ (NA)	✗ (NA)	✗ (NA)
WFG2	2	0.27 (3.0219e+03)	0.33 (6.0751e+03)	0.43 (4.7089e+03)	0.37 (5.6407e+03)	0.37 (4.3414e+03)
	3	✓ (1.4918e+04)	0.70 (3.2334e+04)	✓ (2.2177e+04)#	✓ (2.3527e+04)#	✗ (NA)
WFG2^{-1}	2	✓ (4.3107e+03)	✓ (4.4171e+03)	✓ (4.4526e+03)	✓ (4.5908e+03)#	✓ (4.3400e+03)
	3	0.93 (1.6933e+04)	0.43 (1.5769e+04)	✓ (2.3580e+04)	✓ (2.3414e+04)	✗ (NA)
WFG3	2	✓ (1.0974e+04)	0.13 (3.7698e+03)	✓ (1.4113e+04)#	✓ (1.3696e+04)#	✓ (1.7184e+04)#
	3	✓ (2.4031e+04)#	✗ (NA)	✓ (1.6327e+04)	✓ (1.6975e+04)	✗ (NA)
WFG3^{-1}	2	✓ (6.8804e+03)	0.13 (2.9965e+03)	✓ (7.7343e+03)#	✓ (8.5882e+03)#	✓ (8.1575e+03)#
	3	✗ (NA)	✗ (NA)	✗ (NA)	✗ (NA)	✗ (NA)
VIE1	3	✗ (NA)	✗ (NA)	✓ (9.6216e+02)#	✓ (7.6183e+02)	✗ (NA)
VIE2	3	✓ (1.1300e+02)	✓ (8.1733e+01)	✓ (8.6866e+01)	✓ (1.2800e+02)#	✓ (1.1403e+02)#
VIE3	3	✓ (5.3703e+02)#	✓ (5.3556e+02)#	✓ (4.4373e+02)	✓ (4.9020e+02)#	✓ (4.4970e+02)
LAME $\gamma = 0.25$	2	✓ (2.5740e+02)	✓ (2.9206e+02)	✓ (2.6496e+02)	✓ (2.8333e+02)	✓ (3.1156e+02)#
	3	✓ (7.7591e+02)	✓ (7.9923e+02)#	✓ (7.8209e+02)	✓ (8.0177e+02)#	✓ (8.0298e+02)#
LAME $\gamma = 0.50$	2	✓ (8.0370e+02)	✓ (7.7716e+02)	✓ (7.9970e+02)	✓ (8.3353e+02)#	✓ (8.1173e+02)
	3	✓ (6.3380e+02)#	✓ (6.8466e+02)#	✓ (5.8176e+02)	✓ (6.4490e+02)#	✓ (7.1123e+02)#
LAME $\gamma = 1.00$	2	✓ (1.1465e+03)	✓ (1.1300e+03)	✓ (1.1749e+03)	✓ (1.1643e+03)	✓ (1.2303e+03)#
	3	✓ (1.3446e+03)	✓ (1.3694e+03)	✓ (1.4573e+03)	✓ (1.4124e+03)	✓ (1.7711e+03)#
LAME $\gamma = 2.00$	2	✓ (1.2589e+03)	✓ (1.3292e+03)	✓ (1.2923e+03)	✓ (1.2617e+03)	✓ (1.3706e+03)
	3	✓ (1.6940e+03)	✓ (1.8636e+03)#	✓ (1.7630e+03)	✓ (2.0713e+03)#	✓ (2.2545e+03)#
LAME $\gamma = 5.00$	2	✓ (1.5477e+03)#	✓ (1.3754e+03)	✓ (1.2766e+03)	✓ (1.4851e+03)	✓ (1.3932e+03)
	3	✓ (1.8804e+03)	✓ (2.0437e+03)	✓ (2.1801e+03)	✓ (1.9688e+03)	✓ (2.3004e+03)#
MIRROR $\gamma = 0.25$	2	✓ (1.5231e+03)	✓ (1.2931e+03)	✓ (1.6226e+03)	✓ (1.5719e+03)	✓ (1.3624e+03)
	3	✓ (1.9233e+03)	✓ (2.8885e+03)#	✓ (2.0911e+03)	✓ (3.8951e+03)#	✓ (2.2205e+03)#
MIRROR $\gamma = 0.50$	2	✓ (1.0793e+03)	✓ (1.1544e+03)	✓ (1.1348e+03)	✓ (1.1000e+03)	✓ (1.3918e+03)#
	3	✓ (1.3298e+03)	✓ (1.5272e+03)#	✓ (1.7857e+03)#	✓ (2.4530e+03)#	✓ (3.0045e+03)#
MIRROR $\gamma = 1.00$	2	✓ (1.1329e+03)	✓ (1.0767e+03)	✓ (1.0744e+03)	✓ (1.1544e+03)	✓ (1.0866e+03)
	3	✓ (1.2397e+03)	✓ (1.7526e+03)#	✓ (1.5057e+03)#	✓ (1.5364e+03)#	✓ (1.6742e+03)#
MIRROR $\gamma = 2.00$	2	✓ (9.7663e+02)	✓ (1.0505e+03)	✓ (1.0823e+03)#	✓ (1.0434e+03)	✓ (1.0154e+03)
	3	✓ (1.2303e+03)	✓ (1.3343e+03)	✓ (1.3394e+03)	✓ (1.3497e+03)	✓ (1.3900e+03)#
MIRROR $\gamma = 5.00$	2	✓ (8.6050e+02)	✓ (8.3893e+02)	✓ (9.1160e+02)#	✓ (9.0470e+02)	✓ (8.6323e+02)
	3	✓ (9.3666e+02)	✓ (9.5646e+02)#	✓ (8.7250e+02)	✓ (9.6340e+02)#	✓ (9.1113e+02)

Table 3: Mean and, in parentheses, standard deviation of the Hausdorff distance. The two best values are shown in gray scale, where the darker tone corresponds to the best value. A symbol # is placen when the best algorithm performed significantly better than the others based on a one-tailed Wilcoxon test, using a significance level of $\alpha = 0.05$.

Problema	Dim.	SMS-EMOA	R2-EMOA	IGD$^+$-MaOEA	ϵ^+-MaOEA	Δ_p-MaOEA
DTLZ5	2	3.077574e-02# (1.815526e-03)	9.510878e-03 (1.521790e-04)	6.093201e-02# (9.932257e-03)	5.993075e-02# (1.089149e-02)	1.850188e-02# (2.812982e-03)
	3	3.216520e-02# (1.796077e-03)	7.066692e-02# (3.992978e-02)	5.988385e-02# (1.002451e-02)	5.989544e-02# (1.132659e-02)	1.874597e-02 (3.463474e-03)
DTLZ5^{-1}	2	7.843520e-02# (4.729278e-03)	1.699884e+00# (2.473119e-01)	4.344041e-01# (1.048696e-01)	3.853122e-01# (1.114517e-01)	6.256021e-02 (8.528846e-03)
	3	3.829379e-01 (1.460900e-02)	1.444826e+00# (2.827319e-01)	1.192761e+00# (2.420971e-01)	1.156801e+00# (2.427119e-01)	5.146270e-01# (1.033163e-01)
DTLZ7	2	2.202549e-02 (2.005463e-03)	4.852905e-02# (2.302330e-02)	3.065463e-02# (5.417997e-03)	7.589137e-02# (2.481287e-01)	3.470451e-02 (2.569990e-02)
	3	5.261453e-01# (4.365759e-01)	3.669089e-01 (3.613377e-01)	4.845426e-01# (3.995423e-01)	5.441027e-01# (5.347534e-01)	3.366100e-01 (2.958924e-01)
DTLZ7^{-1}	2	1.187580e-02 (1.004169e-03)	3.711496e-02# (1.834241e-02)	1.761300e-02# (6.396731e-03)	1.807463e-02# (8.560824e-03)	1.302961e-02# (4.361443e-03)
	3	5.481802e-01# (1.776795e-01)	4.797460e-01 (1.518527e-02)	5.339010e-01# (1.174193e-02)	5.750645e-01# (1.711356e-01)	5.522249e-01# (1.795489e-01)
WFG1	2	2.213367e+00 (3.948808e-01)	2.830692e+00# (4.206011e-01)	2.328385e+00# (5.420895e-02)	2.202644e+00# (4.914847e-01)	2.136225e+00# (4.735624e-01)
	3	2.197492e+00 (4.125112e-01)	2.811781e+00# (3.559170e-01)	3.085727e+00# (2.095829e-01)	3.249765e+00# (1.731195e-01)	3.072379e+00# (2.837441e-01)
WFG1^{-1}	2	2.348346e+00# (5.013607e-01)	3.560577e+00# (1.614038e-01)	2.579248e+00# (3.822815e-01)	2.587287e+00# (3.687097e-01)	1.835583e+00 (7.891345e-01)
	3	3.144431e+00 (4.566521e-01)	3.644217e+00# (9.520948e-02)	3.640692e+00# (5.683441e-02)	3.712366e+00# (5.591896e-02)	3.574088e+00# (1.509626e-01)
WFG2	2	7.505522e-01 (4.193102e-01)	7.315594e-01# (3.822844e-01)	6.113520e-01 (4.534472e-01)	6.719010e-01 (4.426562e-01)	6.680274e-01 (4.464939e-01)
	3	1.949492e+00# (1.831101e-01)	1.972061e+00# (8.818055e-02)	2.161069e+00# (1.890187e-01)	2.107503e+00# (1.540904e-01)	1.428000e+00 (3.529359e-01)
WFG2^{-1}	2	2.490296e-02 (1.333398e-03)	1.638632e-01# (8.150410e-02)	4.685722e-02# (8.561709e-03)	4.639651e-02# (7.032178e-03)	4.923717e-02# (8.955797e-03)
	3	1.330635e+00# (8.981255e-02)	7.730115e-01# (6.995659e-02)	9.290884e-01# (1.391188e-01)	9.289295e-01# (8.444951e-02)	6.880378e-01 (7.977693e-02)
WFG3	2	2.707010e-02 (1.121240e-03)	4.011508e-01# (1.575776e-01)	5.339123e-02# (1.394259e-02)	5.038746e-02# (1.123899e-02)	5.753183e-02# (1.266287e-02)
	3	2.108328e+00# (4.214193e-02)	2.124371e+00# (4.720215e-02)	1.490614e+00 (1.557406e-01)	1.445250e+00 (1.461410e-01)	1.723725e+00# (1.199918e-01)
WFG3^{-1}	2	2.466026e-02 (1.343378e-03)	4.682168e-01# (1.769721e-01)	5.507582e-02# (1.385543e-02)	5.835986e-02# (2.302785e-02)	6.257074e-02# (1.894104e-02)
	3	4.196883e-01 (2.153138e-02)	5.821841e-01# (1.038923e-01)	4.439020e-01 (8.330356e-02)	5.805365e-01# (1.639781e-01)	4.858140e-01# (7.909681e-02)
VIE1	3	1.478014e+00# (5.721134e-03)	1.118123e+00# (2.293143e-01)	9.590722e-01 (4.065934e-01)	1.031676e+00 (3.252150e-01)	1.544479e+00# (8.848777e-02)
VIE2	3	7.659238e-02# (1.139953e-02)	4.321739e-01# (1.981138e-01)	5.138187e-01# (2.077573e-01)	5.449889e-01# (2.015539e-01)	6.188452e-02 (1.909836e-02)
VIE3	3	3.597325e+01# (2.535381e-03)	3.580163e+01# (1.483174e-01)	3.570980e+01 (1.239652e-01)	3.580249e+01# (1.644133e-01)	3.596517e+01# (2.413054e-02)
LAME $\gamma = 0.25$	2	7.231123e-02 (1.543747e-03)	7.627063e-01# (9.379871e-02)	4.361314e-01# (5.303411e-02)	4.347943e-01# (7.209262e-02)	1.048069e-01# (1.075039e-02)
	3	3.030839e-01# (6.199006e-02)	8.535220e-01# (2.947354e-01)	7.241131e-01# (2.688209e-02)	7.221472e-01# (3.477759e-02)	1.995764e-01 (3.077426e-02)
LAME $\gamma = 0.50$	2	2.530849e-02# (1.564295e-03)	5.402476e-01# (1.162890e-01)	1.272472e-01# (3.749616e-02)	1.376205e-01# (3.691710e-02)	1.778939e-02 (2.712181e-03)
	3	1.101923e-01# (6.031892e-03)	5.446090e-01# (1.387246e-02)	4.659930e-01# (6.140304e-02)	4.938630e-01# (6.053914e-02)	8.932232e-02 (2.425611e-02)
LAME $\gamma = 1.00$	2	7.589236e-03 (2.965523e-04)	1.007102e-01# (5.897155e-02)	1.313399e-02# (1.948516e-03)	1.329846e-02# (1.638165e-03)	1.973800e-02# (1.835242e-02)
	3	7.173814e-02# (3.872626e-03)	6.206041e-02 (4.862174e-03)	1.050844e-01# (1.151115e-02)	1.179165e-01# (1.197276e-02)	1.111155e-01# (1.292641e-02)
LAME $\gamma = 2.00$	2	3.186574e-02# (1.316612e-03)	1.007065e-02 (3.261561e-04)	6.141609e-02# (9.949159e-03)	5.921995e-02# (8.479438e-03)	1.728853e-02# (2.514175e-03)
	3	1.621467e-01# (4.555663e-03)	9.639930e-02 (2.367559e-04)	1.966129e-01# (2.248088e-02)	1.876308e-01# (2.027803e-02)	1.376867e-01# (1.443447e-02)
LAME $\gamma = 5.00$	2	1.409980e-01# (3.315905e-03)	3.417753e-02 (1.948163e-04)	2.234118e-01# (1.061329e-02)	2.127717e-01# (1.603388e-02)	3.489903e-02# (2.347631e-03)
	3	3.577989e-01# (7.878295e-03)	1.500669e-01 (2.526744e-04)	3.969645e-01# (1.906622e-02)	3.821651e-01# (1.966347e-02)	1.778417e-01# (1.827104e-02)
MIRROR $\gamma = 0.25$	2	1.685054e-01# (3.830728e-03)	4.997593e-02# (5.020421e-05)	2.907454e-01# (1.526963e-02)	2.850196e-01# (1.893000e-02)	4.843340e-02 (1.701295e-03)
	3	2.413126e-01# (4.093401e-03)	9.262397e-02# (9.708269e-03)	3.422523e-01# (1.479797e-02)	3.950458e-01# (1.099417e-01)	4.999952e-02 (5.118307e-03)
MIRROR $\gamma = 0.50$	2	3.741539e-02# (2.082645e-03)	1.035331e-02 (4.401563e-05)	7.385466e-02# (1.007731e-02)	7.193065e-02# (1.092477e-02)	1.851470e-02# (2.759508e-03)
	3	9.976228e-02# (4.064284e-03)	1.124747e-01# (1.086035e-02)	1.379254e-01# (1.743578e-02)	1.642352e-01# (5.671047e-02)	8.372362e-02 (1.921881e-02)
MIRROR $\gamma = 1.00$	2	7.641986e-03 (2.312297e-04)	9.860330e-02# (5.241803e-02)	1.309680e-02# (1.941996e-03)	1.331902e-02# (1.416358e-03)	1.665265e-02# (2.918066e-03)
	3	9.906263e-02 (4.510345e-03)	1.451629e-01# (1.909890e-02)	1.056237e-01 (1.339696e-02)	1.072790e-01# (1.482283e-02)	1.079255e-01# (1.363654e-02)
MIRROR $\gamma = 2.00$	2	2.203991e-02# (1.670770e-03)	4.544187e-01# (7.917778e-02)	9.258290e-02# (2.505483e-02)	1.040329e-01# (3.609639e-02)	1.716760e-02 (2.927445e-03)
	3	1.213664e-01 (4.470778e-03)	3.538615e-01# (3.696266e-02)	3.368791e-01# (4.317780e-02)	3.547486e-01# (4.127689e-02)	1.458980e-01# (1.747558e-02)
MIRROR $\gamma = 5.00$	2	5.878550e-02 (1.711243e-03)	6.881999e-01# (6.701582e-02)	3.174689e-01# (4.997798e-02)	3.425114e-01# (4.141809e-02)	6.861973e-02# (4.090946e-03)
	3	3.402385e-01# (3.222692e-03)	7.875241e-01# (1.882810e-02)	7.533097e-01# (3.185327e-02)	7.785876e-01# (5.575465e-02)	2.116174e-01 (3.172115e-02)

can see from the figure that the distributions of both IGD^+-MaOEA and ϵ^+-MaOEA are not too uniform and their spread is deficient.

4 CONCLUSIONS AND FUTURE WORK

In spite of the broad spectrum of currently available IB-MOEAs, there is still no clear understanding of their convergence and diversity behavior when tackling complex MOPs. In this paper, we performed an empirical analysis of the convergence and diversity properties of five steady-state IB-MOEAs based on the indicators: hypervolume, R2, IGD^+, ϵ^+, and Δ_p, i.e., we analyzed the behavior of SMS-EMOA, R2-EMOA, IGD^+-MaOEA, ϵ^+-MaOEA, and Δ_p-MaOEA. Our study highlights essential insights into the performance of the adopted IB-MOEAs related to their convergence speed, convergence quality of the final Pareto front approximations as well as the uniformity of solutions when tackling MOPs with different Pareto front shapes. The study revealed that, in general, SMS-EMOA speeds up convergence to the Pareto front. However, IGD^+-MaOEA provides convergence results more consistently since it was the IB-MOEA that was able to converge in most of the adopted test instances, although it has a slower convergence than SMS-EMOA. Considering the final convergence quality of the IB-MOEAs, SMS-EMOA is the best algorithm, having the best values in four out six convergence QIs. Regarding diversity, Δ_p-MaOEA produces well-diversified approximation sets in most forms of the Pareto front. In summary, our experimental results allowed us to outline some of the strengths and weaknesses of the IB-MOEAs of our study. As part of our future work, we are interested in studying the effect of the IB-MOEAs on MOPs with several difficulties and on problems with many objective functions, i.e., MOPs with more than three objectives.

ACKNOWLEDGMENTS

The first author acknowledges support from CINVESTAV-IPN and CONACyT to pursue graduate studies in Computer Science and from IEEE Computational Intelligence Society (CIS) for the 2018 IEEE CIS Graduate Student Grant. The second author gratefully acknowledges support from CONACyT grant no. 2016-01-1920 (Investigación en Fronteras de la Ciencia 2016).

REFERENCES

[1] Nicola Beume, Boris Naujoks, and Michael Emmerich. 2007. SMS-EMOA: Multiobjective selection based on dominated hypervolume. *European Journal of Operational Research* 181, 3 (16 September 2007), 1653–1669.
[2] Dimo Brockhoff, Tobias Wagner, and Heike Trautmann. 2012. On the Properties of the *R*2 Indicator. In *2012 Genetic and Evolutionary Computation Conference (GECCO'2012)*. ACM Press, Philadelphia, USA, 465–472. ISBN: 978-1-4503-1177-9.
[3] Dimo Brockhoff, Tobias Wagner, and Heike Trautmann. 2015. R2 Indicator-Based Multiobjective Search. *Evolutionary Computation* 23, 3 (Fall 2015), 369–395.
[4] Carlos A. Coello Coello and Nareli Cruz Cortés. 2002. An Approach to Solve Multiobjective Optimization Problems Based on an Artificial Immune System. In *First International Conference on Artificial Immune Systems (ICARIS'2002)*, Jonathan Timmis and Peter J. Bentley (Eds.). University of Kent at Canterbury, UK, 212–221. ISBN 1-902671-32-5.
[5] Carlos A. Coello Coello, Gary B. Lamont, and David A. Van Veldhuizen. 2007. *Evolutionary Algorithms for Solving Multi-Objective Problems* (second ed.). Springer, New York. ISBN 978-0-387-33254-3.
[6] Kalyanmoy Deb, Amrit Pratap, Sameer Agarwal, and T. Meyarivan. 2002. A Fast and Elitist Multiobjective Genetic Algorithm: NSGA–II. *IEEE Transactions on Evolutionary Computation* 6, 2 (April 2002), 182–197.
[7] Kalyanmoy Deb, Lothar Thiele, Marco Laumanns, and Eckart Zitzler. 2005. Scalable Test Problems for Evolutionary Multiobjective Optimization. In *Evolutionary*

Table 4: Mean and, in parentheses, standard deviation of the Solow-Polasky diversity indicator. The two best values are shown in gray scale, where the darker tone corresponds to the best value. A symbol # is placed when the best algorithm performed significantly better than the others based on a one-tailed Wilcoxon test, using a significance level of $\alpha = 0.05$.

Problema	Dim.	SMS-EMOA	R2-EMOA	IGD^+-MaOEA	ϵ^+-MaOEA	Δ_p-MaOEA
DTLZ5	2	8.799243e+00# (2.420473e-03)	8.817050e+00 (8.601901e-04)	8.692179e+00# (3.515960e-02)	8.698178e+00# (3.673926e-02)	8.799056e+00# (2.640527e-02)
	3	8.802124e+00# (1.842481e-03)	8.539616e+00# (2.631087e-01)	8.699035e+00# (3.573762e-02)	8.698818e+00# (4.114915e-02)	8.806127e+00 (3.350134e-02)
$DTLZ5^{-1}$	2	2.742359e+01 (4.815321e-02)	1.321604e+01# (9.843791e-01)	2.363707e+01# (4.646154e-01)	2.387372e+01# (6.603154e-01)	2.722379e+01# (1.251890e-01)
	3	8.788601e+01# (4.577521e-01)	7.726040e+01# (1.951105e+00)	7.816839e+01# (2.541094e+00)	7.747251e+01# (2.386478e+00)	8.936051e+01 (8.589468e-01)
DTLZ7	2	1.075924e+01# (9.485348e-03)	1.055704e+01# (1.764871e-01)	1.066020e+01# (6.687948e-02)	1.041361e+01# (1.293614e+00)	1.085721e+01 (1.688882e-01)
	3	3.659716e+01# (6.215085e+00)	4.027530e+01# (6.216719e+00)	3.504953e+01# (6.740447e+00)	3.403047e+01# (7.516555e+00)	4.140520e+01 (5.385747e+00)
$DTLZ7^{-1}$	2	6.946015e+00# (4.422645e-03)	6.829293e+00# (1.069516e-01)	6.904642e+00# (4.677685e-02)	6.902470e+00# (4.532370e-02)	6.970949e+00 (3.234239e-02)
	3	2.084053e+01# (3.712756e+00)	2.440047e+01 (1.172822e+00)	2.032370e+01# (5.897520e-01)	1.951134e+01# (3.352975e+00)	2.315315e+01 (4.036582e+00)
WFG1	2	1.154858e+01 (1.062588e+00)	7.966541e+00# (1.461112e+00)	1.095551e+01# (3.125391e-01)	1.122544e+01# (1.345348e+00)	1.174460e+01 (1.270376e+00)
	3	6.254917e+01 (4.372476e+00)	5.412430e+01# (2.518273e+00)	4.603504e+01# (4.082818e+00)	4.426244e+01# (3.908723e+00)	5.570082e+01# (4.245888e+00)
$WFG1^{-1}$	2	1.203741e+01# (1.365288e+00)	5.778459e+00# (8.738993e-01)	1.084528e+01# (1.389314e+00)	1.078942e+01# (1.273548e+00)	1.334489e+01 (1.901042e+00)
	3	5.665910e+01 (2.887329e+00)	4.855241e+01# (1.400438e+00)	5.763648e+01 (3.496319e+00)	5.725661e+01 (3.691241e+00)	5.752122e+01 (3.486851e+00)
WFG2	2	1.997145e+01 (1.973586e+00)	1.926807e+01# (2.128501e+00)	2.028923e+01# (2.203759e+00)	1.995404e+01# (2.181330e+00)	2.046291e+01 (2.145987e+00)
	3	6.717654e+01# (7.372088e-01)	8.027439e+01# (6.586682e-01)	6.535570e+01# (2.440267e+00)	6.372450e+01# (2.121404e+00)	8.892057e+01 (1.556707e+00)
$WFG2^{-1}$	2	2.078503e+01 (5.416172e-03)	1.977792e+01# (4.077274e-01)	2.059536e+01# (4.728328e-02)	2.061597e+01# (5.553223e-02)	2.057292e+01# (3.591416e-02)
	3	8.602704e+01# (4.711341e-01)	8.723124e+01# (1.551029e+00)	8.456642e+01# (1.814969e+00)	8.448289e+01# (2.090042e+00)	9.829389e+01 (7.357824e-01)
WFG3	2	2.296039e+01 (1.291320e-02)	1.963773e+01# (1.165537e+00)	2.249084e+01# (1.543758e-01)	2.255296e+01# (1.258089e-01)	2.248167e+01# (1.233345e-01)
	3	5.567263e+01# (5.521267e-01)	6.133350e+01# (2.321322e+00)	5.456024e+01# (2.082674e+00)	5.449212e+01# (2.207354e+00)	6.617536e+01 (2.082402e+00)
$WFG3^{-1}$	2	2.297874e+01 (6.553550e-03)	1.940599e+01# (1.115155e+00)	2.249152e+01# (1.306431e-01)	2.244912e+01# (1.858592e-01)	2.244101e+01# (1.810237e-01)
	3	8.841161e+01# (3.785907e-01)	7.898779e+01# (1.483873e+00)	9.134386e+01 (6.203059e-01)	9.023680e+01# (8.485443e-01)	8.936711e+01# (7.411444e-01)
VIE1	3	6.805718e+01# (2.521458e-01)	6.740573e+01# (2.310275e+00)	5.453501e+01# (1.807842e+00)	5.552227e+01# (1.601203e+00)	8.005502e+01 (1.007591e+00)
VIE2	3	1.154615e+01# (8.125594e-02)	8.685414e+00# (7.102800e-01)	7.650740e+00# (6.617115e-01)	7.504154e+00# (6.006657e-01)	1.206634e+01 (1.333495e-01)
VIE3	3	2.270243e+01# (5.071533e-01)	2.839043e+01# (3.382631e+00)	3.244248e+01# (1.354320e+00)	3.226683e+01# (1.642415e+00)	4.040227e+01 (7.245011e-01)
LAME $\gamma = 0.25$	2	8.941437e+00# (5.772376e-02)	3.466396e+00# (7.335002e-01)	5.424995e+00# (4.050875e-01)	5.319769e+00# (5.079335e-01)	1.034601e+01 (8.009878e-02)
	3	8.305585e+00# (4.656517e-01)	3.211022e+00# (4.651394e+00)	3.245153e+00# (4.269564e-01)	3.169452e+00# (5.650221e-01)	1.526692e+01 (2.753743e-01)
LAME $\gamma = 0.50$	2	9.048334e+00 (2.749814e-03)	4.986518e+00# (6.211100e-01)	7.998533e+00# (3.082688e-01)	7.950827e+00# (2.356451e-01)	9.036493e+00# (4.215163e-02)
	3	1.564823e+01# (7.329384e-02)	7.704771e+00# (2.898069e-01)	9.790586e+00# (9.073317e-01)	9.538096e+00# (7.712106e-01)	1.653927e+01 (3.867472e-01)
LAME $\gamma = 1.00$	2	8.058952e+00 (4.966752e-05)	7.331385e+00# (4.002672e-01)	8.023044e+00# (2.398873e-02)	8.023164e+00# (2.213841e-02)	8.057805e+00# (1.033550e-01)
	3	2.323513e+01 (2.566032e-02)	2.237926e+01# (1.294749e-01)	2.128746e+01# (3.254218e-01)	2.098928e+01# (4.041683e-01)	2.221247e+01# (4.165485e-01)
LAME $\gamma = 2.00$	2	8.798746e+00# (2.632126e-03)	8.816465e+00 (8.420813e-04)	8.686890e+00# (3.921337e-02)	8.694720e+00# (3.146748e-02)	8.783966e+00# (1.916459e-02)
	3	3.186759e+01# (9.079239e-02)	3.339525e+01 (4.378280e-02)	3.023575e+01# (3.969481e-01)	3.043253e+01# (4.591035e-01)	3.098430e+01# (4.273541e-01)
LAME $\gamma = 5.00$	2	8.877808e+00# (4.605688e-02)	9.919260e+00 (1.664460e-03)	7.541355e+00# (1.632247e-01)	7.715249e+00# (1.916045e-01)	9.879156e+00# (3.017395e-02)
	3	2.502635e+01# (1.259251e-01)	4.221664e+01 (1.023175e-02)	2.400398e+01# (6.107517e-01)	2.512005e+01# (7.301891e-01)	3.861530e+01# (7.545026e-01)
MIRROR $\gamma = 0.25$	2	8.841968e+00# (4.921558e-02)	1.036926e+01 (1.776357e-15)	6.736968e+00# (1.987818e-01)	6.823645e+00# (2.712274e-01)	1.030823e+01# (3.404778e-02)
	3	1.093615e+01# (8.161102e-02)	1.416913e+01# (1.578056e-01)	8.310661e+00# (2.339188e-01)	8.203387e+00# (4.731011e-01)	1.477297e+01 (1.127953e-01)
MIRROR $\gamma = 0.50$	2	9.041054e+00# (3.636536e-03)	9.073550e+00 (7.303778e-04)	8.864132e+00# (5.197892e-02)	8.861065e+00# (6.512181e-02)	9.012983e+00# (3.688009e-02)
	3	1.697328e+01 (2.304582e-02)	1.640375e+01# (9.601057e-02)	1.587693e+01# (1.940042e-01)	1.557452e+01# (4.660800e-01)	1.606433e+01# (2.022736e-01)
MIRROR $\gamma = 1.00$	2	8.058956e+00 (4.227378e-05)	7.351128e+00# (3.632428e-01)	8.019590e+00# (2.783349e-02)	8.020846e+00# (2.282434e-02)	8.010456e+0#0 (3.325008e-02)
	3	2.359319e+01 (2.318634e-02)	2.190992e+01# (2.844364e-01)	2.227936e+01# (3.610438e-01)	2.217250e+01# (3.822628e-01)	2.134092e+01# (3.833550e-01)
MIRROR $\gamma = 2.00$	2	8.799740e+00 (1.840336e-03)	4.916376e+00# (3.814669e-01)	7.952831e+00# (2.387585e-01)	7.866694e+00# (2.710103e-01)	8.736439e+00# (4.902078e-02)
	3	3.162068e+01 (3.684369e-02)	2.706497e+01# (6.640911e-01)	2.126063e+01# (1.065545e+00)	2.087369e+01# (1.212016e+00)	2.952776e+01# (5.195778e-01)
MIRROR $\gamma = 5.00$	2	8.713909e+00# (4.863761e-02)	2.961759e+00# (3.079325e-01)	6.252545e+00# (3.950805e-01)	6.073869e+00# (3.581654e-01)	9.810047e+00 (5.141206e-02)
	3	2.442199e+01# (1.206717e-01)	1.850840e+01# (8.730292e-01)	1.260572e+01# (1.243608e+00)	1.200266e+01# (1.300137e+00)	3.611698e+01 (7.843774e-01)

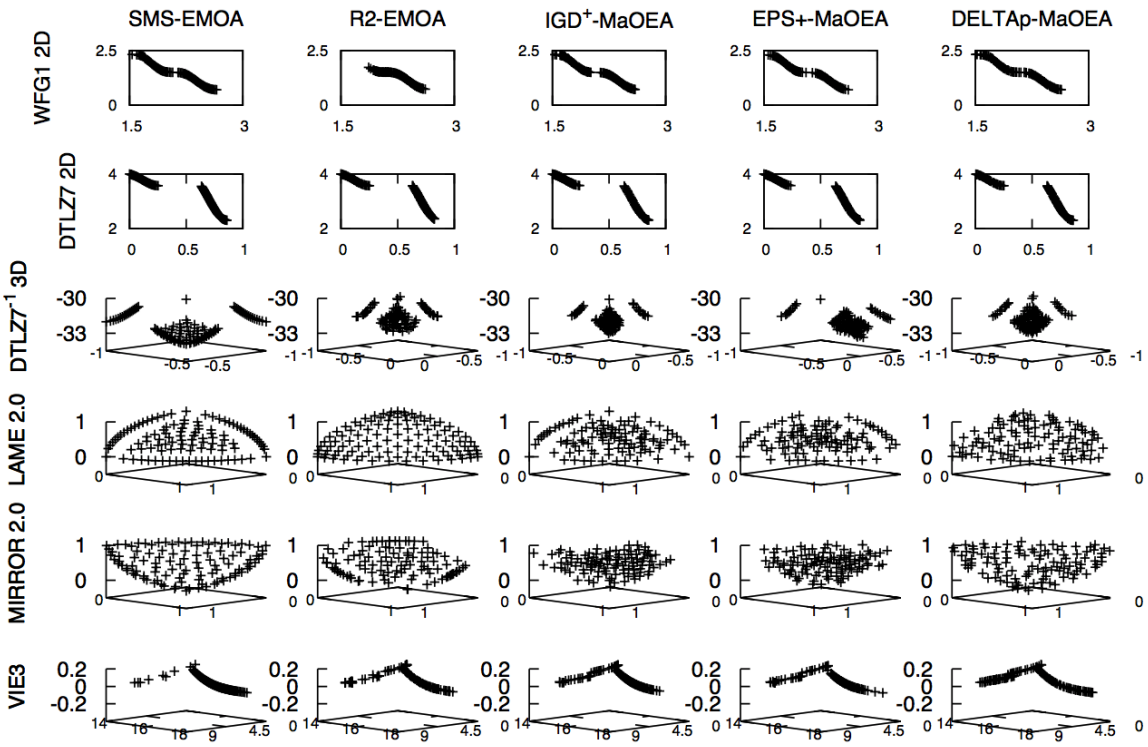

Figure 3: Approximated Pareto fronts produced by all the adopted IB-MOEAs. Each approximation set corresponds to the median of the Solow-Polasky Diversity indicator.

Multiobjective Optimization. Theoretical Advances and Applications, Ajith Abraham, Lakhmi Jain, and Robert Goldberg (Eds.). Springer, USA, 105–145.

[8] Michael T.M. Emmerich and André H. Deutz. 2007. Test Problems Based on Lamé Superspheres. In *Evolutionary Multi-Criterion Optimization, 4th International Conference, EMO 2007*, Shigeru Obayashi, Kalyanmoy Deb, Carlo Poloni, Tomoyuki Hiroyasu, and Tadahiko Murata (Eds.). Springer. Lecture Notes in Computer Science Vol. 4403, Matshushima, Japan, 922–936.

[9] Michael T.M. Emmerich, André H. Deutz, and Johannes W. Kruisselbrink. 2013. On Quality Indicators for Black-Box Level Set Approximation. In *EVOLVE - A bridge between Probability, Set Oriented Numerics and Evolutionary Computation*, Emilia Tantar, Alexandru-Adrian Tantar, Pascal Bouvry, Pierre Del Moral, Pierrick Legrand, Carlos A. Coello Coello, and Oliver Schütze (Eds.). Springer-Verlag. Studies in Computational Intelligence Vol. 447, Heidelberg, Germany, Chapter 4, 157–185. 978-3-642-32725-4.

[10] Jesús Guillermo Falcón-Cardona and Carlos A. Coello Coello. 2018. Towards a More General Many-objective Evolutionary Optimizer. In *Parallel Problem Solving from Nature – PPSN XV, 15th International Conference, Proceedings, Part I*. Springer. Lecture Notes in Computer Science Vol. 11101, Coimbra, Portugal, 335–346. ISBN: 978-3-319-99258-7.

[11] D. P. Hardin and E. B. Saff. [n. d.]. Discretizing Manifolds via Minimum Energy Points. *Notices of the AMS* 51, 10 ([n. d.]), 1186–1194.

[12] Simon Huband, Phil Hingston, Luigi Barone, and Lyndon While. 2006. A Review of Multiobjective Test Problems and a Scalable Test Problem Toolkit. *IEEE Transactions on Evolutionary Computation* 10, 5 (October 2006), 477–506.

[13] Hisao Ishibuchi, Hiroyuki Masuda, Yuki Tanigaki, and Yusuke Nojima. 2015. Modified Distance Calculation in Generational Distance and Inverted Generational Distance. In *Evolutionary Multi-Criterion Optimization, 8th International Conference, EMO 2015*, António Gaspar-Cunha, Carlos Henggeler Antunes, and Carlos Coello Coello (Eds.). Springer. Lecture Notes in Computer Science Vol. 9019, Guimarães, Portugal, 110–125.

[14] Hisao Ishibuchi, Yu Setoguchi, Hiroyuki Masuda, and Yusuke Nojima. 2017. Performance of Decomposition-Based Many-Objective Algorithms Strongly Depends on Pareto Front Shapes. *Trans. Evol. Comp* 21, 2 (April 2017), 169–190.

[15] Siwei Jiang, Yew-Soon Ong, Jie Zhang, and Liang Feng. 2014. Consistencies and Contradictions of Performance Metrics in Multiobjective Optimization. *IEEE Transactions on Cybernetics* 44, 12 (December 2014), 2391–2404.

[16] Joshua Knowles and David Corne. 2002. On Metrics for Comparing Nondominated Sets. In *Congress on Evolutionary Computation (CEC'2002)*, Vol. 1. IEEE Service Center, Piscataway, New Jersey, 711–716.

[17] Arnaud Liefooghe and Bilel Derbel. 2016. A Correlation Analysis of Set Quality Indicator Values in Multiobjective Optimization. In *2016 Genetic and Evolutionary Computation Conference (GECCO'2016)*. ACM Press, Denver, Colorado, USA, 581–588. ISBN 978-1-4503-4206-3.

[18] N. Riquelme, C. Von Lücken, and B. Baran. 2015. Performance metrics in multiobjective optimization. In *2015 Latin American Computing Conference (CLEI)*. IEEE press, 1–11.

[19] Oliver Schütze, Xavier Esquivel, Adriana Lara, and Carlos A. Coello Coello. 2012. Using the Averaged Hausdorff Distance as a Performance Measure in Evolutionary Multiobjective Optimization. *IEEE Transactions on Evolutionary Computation* 16, 4 (August 2012), 504–522.

[20] David A. Van Veldhuizen. 1999. *Multiobjective Evolutionary Algorithms: Classifications, Analyses, and New Innovations*. Ph.D. Dissertation. Department of Electrical and Computer Engineering. Graduate School of Engineering. Air Force Institute of Technology, Wright-Patterson AFB, Ohio, USA.

[21] David A. Van Veldhuizen and Gary B. Lamont. 1999. Multiobjective Evolutionary Algorithm Test Suites. In *Proceedings of the 1999 ACM Symposium on Applied Computing*, Janice Carroll, Hisham Haddad, Dave Oppenheim, Barrett Bryant, and Gary B. Lamont (Eds.). ACM Press, San Antonio, Texas, 351–357.

[22] Qingfu Zhang and Hui Li. 2007. MOEA/D: A Multiobjective Evolutionary Algorithm Based on Decomposition. *IEEE Transactions on Evolutionary Computation* 11, 6 (December 2007), 712–731.

[23] Eckart Zitzler and Lothar Thiele. 1998. Multiobjective Optimization Using Evolutionary Algorithms—A Comparative Study. In *Parallel Problem Solving from Nature V*, A. E. Eiben (Ed.). Springer-Verlag, Amsterdam, 292–301.

[24] Eckart Zitzler, Lothar Thiele, Marco Laumanns, Carlos M. Fonseca, and Viviane Grunert da Fonseca. 2003. Performance Assessment of Multiobjective Optimizers: An Analysis and Review. *IEEE Transactions on Evolutionary Computation* 7, 2 (April 2003), 117–132.